JOC The Journal of Organic Chemistry

Note

Kinetics and Thermodynamics of Binding Between Zwitterionic Viologen Guests and the Cucurbit[7]uril Host

Yeting Zheng, and Angel E. Kaifer

J. Org. Chem., **Just Accepted Manuscript** • DOI: 10.1021/acs.joc.0c01201 • Publication Date (Web): 13 Jul 2020

Kinetics and Thermodynamics of Binding Between Zwitterionic Viologen Guests and the Cucurbit[7]uril Host

Yeting Zheng and Angel E. Kaifer*

Department of Chemistry, University of Miami, Coral Gables, FL 33124, U.S.A.

Supporting Information Placeholder

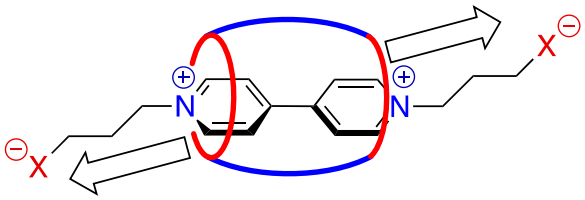

ABSTRACT: The host-guest binding interactions between a series of zwitterionic, symmetric viologens and the cucurbit[7]uril host were investigated using NMR and UV-Vis spectroscopic techniques. The nature of the viologen side arms had strong effects on the kinetics of association and dissociation and weaker, more uniform influence on the thermodynamic stability of the final 1:1 inclusion complexes, which can also be characterized as pseudorotaxanes.

Viologens is the common name applied to the family of diquaternized 4,4'-bipyridinium cations.[1] Simple viologens[2-3] were among the first guests proposed for the cucurbit[7]uril (CB[7]) host (see Figure 1 for structure) shortly after its initial discovery and isolation.[4] These binding interactions may lead to two different types of inclusion complexes,[5] depending on the main binding site for the host, either the central bipyridinium nucleus or one of the terminal *N*-substituents or side arms. As a result, CB[7] binding interactions with viologens have been used in a number of applications.[6-25] Our group has investigated viologen guests with aliphatic side arms terminated on carboxylic acid groups,[26] finding that the predominant binding site for CB[7] is the viologen nucleus when the terminal carboxylates are deprotonated. However, upon protonation of the carboxylates, CB[7] shuttles back and forth between the two aliphatic side arms. Later on, we investigated the kinetics of dissociation of these CB[7] complexes and found very slow dissociation rates when the carboxylates are deprotonated.[27] In general, these binding phenomena were understood as the result of the repulsive interactions between the negatively charged COO^- groups and the cavity entrances (portals) of the CB[7] host, which are lined with carbonyl oxygens.[28] More recently, we have also investigated the binding interactions between CB[7] and a series of guests containing a central bis(pyridinium)-xylylene site and terminal carboxylate groups.[29]

The few binding pairs between CB[7] and carboxylate-terminated guests offer small variations in the thermodynamic stability of the final inclusion complexes and large variations on the association and dissociation kinetic rate constants depending on the nature and structure of the side arms. Intrigued by this uncommon feature, we decided to investigate more systematically the kinetics and thermodynamics of binding between CB[7] and

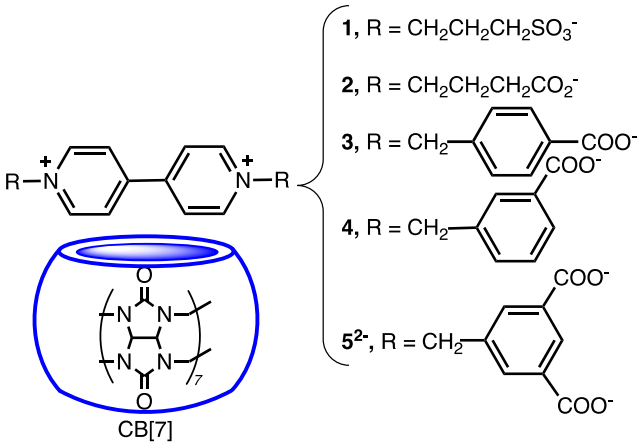

Figure 1. Structures of the CB[7] host and the viologen guests surveyed in this work.

a series of viologen guests designed to assess the effects of the side arm structure and terminal groups on the binding process. The selected series of viologen guests is shown in Figure 1. This research work may lead to a deeper understanding of the dynamics of CB[n]-based rotaxanes and pseudorotaxanes.

CB[7] was synthesized according to a published procedure[30] and its purity was assessed by a method previously reported by our group.[31] The synthesis of the viologen guests is relatively straightforward, essentially following reported procedures for the same or similar compounds (see Experimental Section). All

experiments were done in 50 mM NaCl solutions, adjusted to a final pH in the range 7.5-8 by small aliquot additions of NaOH (or NaOD in the NMR spectroscopic experiments). The solution pH value was selected to fully drive the deprotonation of all the terminal groups on the side arms, ensuring that the guests were well represented by the structures shown on Figure 1. With guests **1** to **4**, NMR spectroscopic data clearly supported the formation of inclusion complexes in which the CB[7] host encircles the central bipyridinium nucleus, as evidenced primarily by a pronounced upfield shift on the resonance of this group's β (inner) protons.[3] Therefore, the corresponding complexes can be described as pseudorotaxanes. We could not find any evidence for stable complex formation between $\mathbf{5}^{2-}$ and CB[7] (vide infra). The complexation of any of the guests **1-4** and CB[7] can also be monitored by UV-Vis spectroscopy, as the inclusion of the viologen nucleus inside the host results in a depressed absorption of the characteristic band of these compounds around 260 nm. For instance, Figure 2A shows the kinetics measured at 261 nm for guest **1** after addition of 1.0 equivalent of CB[7]. Since the host does not absorb light in this wavelength region, the observed absorbance variation is ascribed to the gradual conversion of free **1** to the **1**@CB[7] complex. These plots were also used to determine the time required to reach the complexation equilibrium points, which was particularly important for the determination of the overall equilibrium association constants (*K* values).

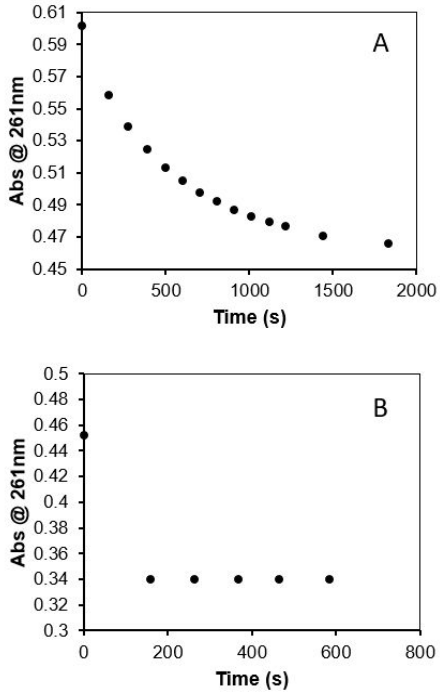

Figure 2. Time dependence of the absorbance at 261 nm for equimolar mixtures of CB[7] plus (A) guest **1** and (B) guest **2**. Guest concentration: 25 μM.

Notice that the complexation process is much faster for guest **2**, as the limiting absorbance value for the inclusion complex is reached in less than 2 minutes, and the association kinetics is so fast that we could not record any intermediate stages for the complexation process.

By titrating a guest solution with gradually increasing concentrations of the CB[7] host we could fit the resulting absorbance data to a 1:1 binding isotherm in order to extract the corresponding *K* values.[3] Illustrative examples are given in the supporting information. The resulting *K* values (Table 1) are all relatively close to one another, with a maximum value of 1.5 x 10^5 M^{-1} and a minimum value of 3.1 x 10^4 M^{-1}. This finding reflects the fact that, in the complexes, CB[7] is always located around the viologen nucleus. Since the binding station is the same regardless of the structure of the side arms, the rather small variations on the measured *K* values primarily reflect minor repulsive interactions between the negatively charged terminal groups and the oxygen-laced CB[7] portals.

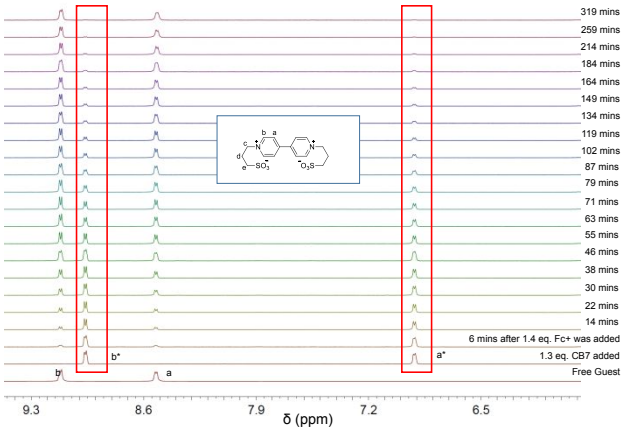

Figure 3. Time dependence of the ^{1}H NMR spectrum of **1**@CB[7] after the addition of 1.4 equiv of Fc^+. All spectra (500 MHz) were recorded in 50 mM NaCl/D_2O with pD adjusted to 8. For clarity reasons, only the aromatic protons are shown.

In order to investigate the dissociation kinetics of these complexes, we carried out experiments in which a given viologen@CB[7]complex was exposed to ca. 1.5 equivalents of (ferrocenylmethyl)trimethylammonium (Fc^+). This cationic guest shows a much higher binding affinity with CB[7] than any of the guests surveyed here. In fact, the equilibrium association constant of CB[7] with Fc^+ is about six orders of magnitude larger that those of the zwitterionic guests surveyed here,[32-33] guaranteeing a large thermodynamic driving force for the dissociation process. Therefore, by monitoring the NMR spectrum of the complex as a function of time after the addition of Fc^+, we can follow the time evolution of the concentrations of bound and free viologen guest, thus allowing the determination of the dissociation rate constant (k_{OUT}).[34-35] For instance, Figure 3 shows the time-dependent ^{1}H NMR spectra obtained in the case of the **1**@CB[7] complex. The aromatic proton signals of the bipyridinium nucleus (a, b) provide a nice handle to follow the decomplexation process. By measuring the gradually decreasing integrated intensities for the β proton signal (a*) and the increasing intensities for the same proton in the free guest (a), we collected data points for the determination of k_{OUT} (See S.I. for more details). Clearly, the dissociation proceeds slowly in this case, presumably because of the electrostatic barrier created by the terminal sulfonate groups.

We have already used the same methodology in previous work.[27, 29] Finally, the apparent association rate constants (k_{IN}) were determined as the product of *K* and k_{OUT}. The resulting values are collected in Table 1.

Table 1. Thermodynamic and kinetic parameters at 25°C for the CB[7] complexes of guests 1-4 in 50 mM NaCl at pH 7.5-8.

Guest	K,[a] M^{-1}	k_{IN}, $M^{-1}s^{-1}$	k_{OUT}, s^{-1}
1	6.0 x 10^4	1.3 x 10^1	2.1 x 10^{-4}
2	6.9 x 10^4	Fast	Fast
3	1.5 x 10^5	1.1 x 10^2	7.0 x 10^{-4}
4	3.1 x 10^4	1.6 x 10^2	5.3 x 10^{-3}

[a]Error margins estimated at ±15%

The results were surprising in a number of ways. First, the contrast between guests **1** and **2** is striking. While the thermodynamic stability of both complexes is similar (ΔG^0 values of -27.3 and -27.6 kJ mol^{-1}, respectively) their kinetic parameters are very different. With guest **2**, the dissociation was too fast to measure by NMR experiments. Both guests are structurally identical, with the single exception of their terminal groups, $-SO_3^-$ in **1** and $-CO_2^-$ in **2**, which must be responsible for the observed kinetic rate differences. In particular, the k_{OUT} value for **2**@CB[7] is estimated to be at least 1 x 10^{-2} s^{-1} or higher, based on the fact that no more than 5% of the complex remains after 5 min of exposure to Fc^+. Therefore, the rate of CB[7] dissociation is about two orders of magnitude slower for the sulfonate-terminated viologen guest than for the carboxylate-terminated viologen guest. This interesting finding suggests that the shapes of the terminal groups are significant, and that a negative charge delocalized over three oxygen atoms at the base of the tetrahedral $-SO_3^-$ group creates a higher electrostatic barrier to the passage of the host than the trigonal planar $-CO_2^-$ group.

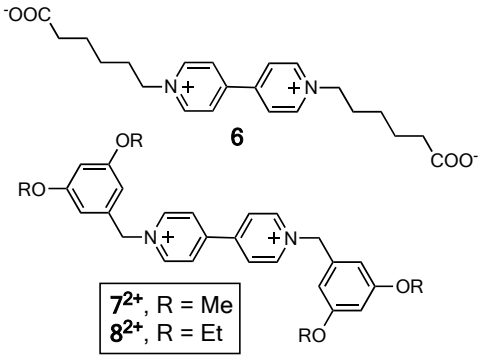

Figure 4. Structure of related viologen guests surveyed in previous work.

It is also important to compare the relatively fast dissociation kinetics of **2**@CB[7] with the much slower kinetics previously measured by us with a very similar viologen guest (compound **6** in Figure 4), in which the side arms were just two methylenes longer than in guest **2**.[27] A suitable rationalization for this difference may involve the possibility of CB[7] residing around the longer sidearm (five methylenes long) forming a metastable complex, which might delay the host passage over the terminal carboxylate group. The formation of a similar metastable complex would not be possible with guest **2**, as the sidearms are only three methylenes long, clearly too short to accommodate the length of the host cavity. A more complete elucidation of these structural issues and their effects on the dissociation kinetics may require a more detailed study focused on side arm length.

A comparison between the measured kinetic rate constants for guests **3** and **4** shows faster kinetics for the latter compound. This finding indicates that the location of the carboxylate groups on *meta* positions relative to the main axle of the guest leads to faster dissociation and association processes compared to the same guest with *para* carboxylate groups. We have observed the same trend in CB[7] binding studies with guest compounds containing a central bis(pyridinium)-xylylene site.[29] A reasonable explanation for the kinetic differences takes into account the closer proximity on the *meta* compound between the negatively charged carboxylates and the corresponding positively charged nitrogens, as compared to the same distance on the *para* compound. The closer proximity between the opposing charges diminishes the overall effect of the negative charge, thus lowering the electrostatic barrier for passage of the CB[7] host (with its carbonyl oxygen-laced portals). At the same time, the closer proximity between the charges on compound **4** also lowers slightly the overall thermodynamic stability of its CB[7] complex as compared to that for **3**@CB[7] (see K values in Table 1), as the complex stabilization resulting from the positively charged nitrogens is decreased as well.

We must also emphasize here that compound $\mathbf{5}^{2-}$ is not bound by CB[7] as evidenced by NMR and UV-Vis spectroscopic experiments, showing the invariance of the corresponding spectra hours after exposure to the CB[7] host (Figure S7). These findings contrast with our previous report on the complexation of the corresponding methyl and ethyl tetraether compounds (compounds $\mathbf{7}^{2+}$ and $\mathbf{8}^{2+}$ in Figure 4).[36] In D_2O solution, the methyl ether undergoes fast complexation with CB[7], while the association with the ethyl ether is slower and can be monitored by NMR experiments, taking several hours to reach equilibrium. Clearly, these results suggest that the lack of binding between $\mathbf{5}^{2-}$ and CB[7] is not due to steric hindrance, but to the electrostatic barrier that the two carboxylates on each of the guest's side arm ends presents to the approach and threading of CB[7].

Scheme 1. Representative sketch of the energetics as CB[7] slides along the guest's molecular axle.

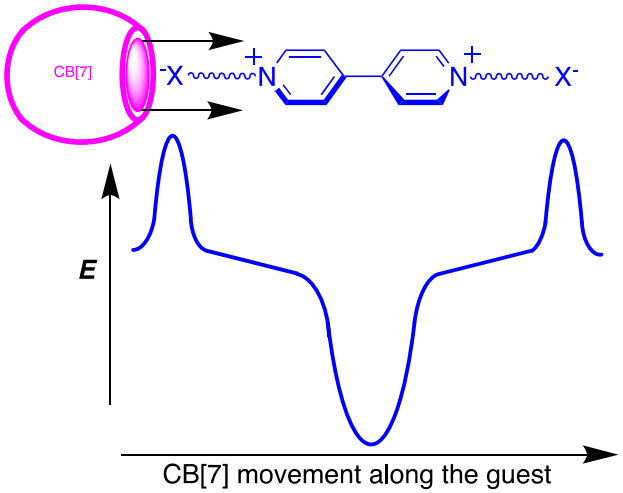

The results obtained in this work clearly reveal that the electrostatic repulsions between negatively charged terminal groups on the guest and the carbonyl-laced portals of the host play relatively minor roles on the thermodynamic stability of the resulting complexes. In fact, the CB[7] complexes with guests **1-4** are all less stable than the complexes formed between the same host and methyl viologen or other simple viologens. In other words, the central energy well in Scheme 1 is associated with the formation of pseudorotaxane-type complexes for all the surveyed guests. However, the kinetic rates of association and dissociation are strongly affected by the nature (sulfonate *vs* carboxylate) and positioning of the negatively charged terminal groups, such as meta *vs* para substitution on the terminal benzyl groups, which define the height of the energy barriers at both axle ends (Scheme 1). The findings in this work can be useful to the design of supramolecular systems with variable or controlled rates of dissociation, which may be of interest in drug delivery,[22, 37-40] among other applications.

EXPERIMENTAL SECTION

*Synthesis of **1***. A mixture of 4,4'-Bipyridine (0.78 g, 5.0 mmol) and 1,3-propanesultone (1.5 g, 12 mmol) was refluxed (oil bath) at 120 °C for 15 min under nitrogen. To the resulting semi-solid mixture, DMSO (5 mL) was added and heated to 120 °C for 3 h under continuous stirring. After cooling, the white precipitate was filtered off and washed several times with methanol and dried over filter paper to give 77% yield of the desired product. The ^{1}H NMR spectrum matched that reported in the literature.[41]

*Synthesis of **2**•Br_2*. 4,4'-Bipyridine (2.0 g, 12.8 mmol) and ethylbromobutyrate (9.98 g, 51.2 mmol) were refluxed (oil bath) in acetonitrile (50 mL) for 28 h. The resulting precipitate was filtered out, washed with Et_2O and recrystallized from MeOH-Et_2O to afford the yellow diethyl ester. This product was dissolved in 2M HBr (15 mL) and left standing for two days. The mixture was then poured into acetone (50 mL) and filtered off. The precipitate was washed with acetone (3 x 35 mL) and dried under vacuum. The ^{1}H NMR spectrum matched that reported in the literature.[42-43]

*Synthesis of **3**•Cl_2*. 4,4'-Bipyridine (3.12 g, 20 mmol) and 4-(chloromethyl)benzoic acid (6.824 g, 40 mmol) were dissolved in DMF (15 mL) and stirred at 120 °C (oil bath) under nitrogen for 4 h. After cooling, the resulting precipitate was filtered off, washed with DMF and dried under vacuum to give the desired product as a white powder (35% yield). The ^{1}H NMR spectrum matched that reported in the literature.[44]

*Synthesis of **4**•Cl_2*. 4,4'-Bipyridine (2.0 g, 12.8 mmol) and 3-(chloromethyl)benzoic acid (6.56 g, 38.4 mmol) were dissolved in DMF (13 mL) and stirred at 120 °C (oil bath) under nitrogen for 8 h. After cooling, the resulting yellow precipitate was isolated by filtration and washed with hot DMF three times. The product was recrystallized with acetone and deionized water (1:1 v/v) to give a pale yellow solid (89% yield). The ^{1}H NMR spectrum matched that reported in the literature.[45]

*Synthesis of **5**•Br_2*. 4,4'-Bipyridine (1.0 g, 6.40 mmol) and dimethyl 5-(bromomethyl)isophthalate[46] (3.67 g, 12.8 mmol) were refluxed (oil bath) in CH_3CN (15 mL) for 24 h. After cooling, the resulting yellow precipitate was collected by filtration, washed with CH_3CN and dried in vacuum to give the tetramethyl ester as a light yellow solid (80% yield). This product (1.00 g, 1.37 mmol) was dissolved in concentrated HBr (30 mL) and refluxed (oil bath) for 2 days. At that point the solution was slowly cooled to room temperature and placed in a refrigerator (2 °C) for 12 h. The resulting white precipitate was filtered off, washed with water and acetone and dried under vacuum. The ^{1}H NMR spectrum matched that reported in the literature.[47]

The pH (or pD) of all solutions was adjusted before any measurements to the desired range (7.5-8.0) by addition of small aliquots of concentrated solutions of NaOH (or NaOD) and then measured with a pH meter. All the solutions contain 50 mM NaCl in order to insure that the concentration of Na^+ does not change significantly when adjusting the pH.

ASSOCIATED CONTENT

Supporting Information

^{1}H NMR spectra of all guests, UV-Vis titrations for binding constant determinations, ^{1}H NMR data for kinetic measurements and determination of dissociation rate constants (PDF file). The Supporting Information is available free of charge on the ACS Publications website.

AUTHOR INFORMATION

Corresponding Author

*Angel E. Kaifer, Department of Chemistry, University of Miami, Coral Gables, FL 33124, U.S.A. E-mail: akaifer@miami.edu

Author Contributions

The manuscript was written through contributions of all authors, and all authors have given approval to the final version of the manuscript.

ACKNOWLEDGMENT

The authors are grateful to the U.S. National Science Foundation for the generous support of this work (to AEK, CHE-1412455). We thank Mehdi Rashvand Avei for assistance with the determination of binding constants.

REFERENCES

1. Monk, P. M. S., *The Viologens : Physicochemical Properties, Synthesis, and Applications of the Salts of 4,4'-Bipyridine*. Wiley: Chichester ; New York, 1998; p xix, 311 p.
2. Kim, H. J.; Jeon, W. S.; Ko, Y. H.; Kim, K., Inclusion of Methylviologen in Cucurbit[7]uril. *Proc. Nat. Acad. Sci. USA* **2002**, *99* (8), 5007-5011.
3. Ong, W.; Gomez-Kaifer, M.; Kaifer, A. E., Cucurbit[7]uril: A Very Effective Host for Viologens and Their Cation Radicals. *Org. Lett.* **2002**, *4* (10), 1791-1794.
4. Kim, J.; Jung, I. S.; Kim, S. Y.; Lee, E.; Kang, J. K.; Sakamoto, S.; Yamaguchi, K.; Kim, K., New Cucurbituril Homologues: Syntheses, Isolation, Characterization, and X-ray Crystal Structures of Cucurbit[n]uril (n=5, 7, and 8). *J. Am. Chem. Soc.* **2000**, *122* (3), 540-541.
5. Moon, K.; Kaifer, A. E., Modes of Binding Interaction between Viologen Guests and the Cucurbit[7]uril Host. *Org. Lett.* **2004**, *6* (2), 185-188.
6. Mal, A.; Vijayakumar, S.; Mishra, R. K.; Jacob, J.; Pillai, R. S.; Kumar, B. S. D.;

Ajayaghosh, A., Supramolecular Surface Charge Regulation in Ionic Covalent Organic Nanosheets: Reversible Exfoliation and Controlled Bacterial Growth. *Angew. Chem. Int. Ed.* **2019**, *58*, 2-9.
7. Liu, Y.; Li, X. Y.; Zhang, H. Y.; Li, C. J.; Ding, F., Cyclodextrin-driven Movement of Cucurbit[7]uril. *J. Org. Chem.* **2007**, *72* (10), 3640-3645.
8. Yuan, L.; Wang, R. B.; Macartney, D. H., Binding modes of Cucurbit[6]uril and Cucurbit[7]uril with a Tetracationic Bis(viologen) Guest. *J. Org. Chem.* **2007**, *72* (12), 4539-4542.
9. Vincil, G. A.; Urbach, A. R., Effects of the Number and Placement of Positive Charges on Viologen-cucurbit[n]uril Interactions. *Supramol. Chem.* **2008**, *20* (8), 681-687.
10. Freitag, M.; Gundlach, L.; Piotrowiak, P.; Galoppini, E., Fluorescence Enhancement of Di-p-tolyl Viologen by Complexation in Cucurbit[7]uril. *J. Am. Chem. Soc.* **2012**, *134* (7), 3358-3366.
11. Kalmar, J.; Ellis, S. B.; Ashby, M. T.; Halterman, R. L., Kinetics of Formation of the Host-Guest Complex of a Viologen with Cucurbit[7]uril. *Org. Lett.* **2012**, *14* (13), 3248-3251.
12. Singh, A.; Yip, W. T.; Halterman, R. L., Fluorescence-On Response via CB7 Binding to Viologen-Dye Pseudorotaxanes. *Org. Lett.* **2012**, *14* (16), 4046-4049.
13. Zhu, L. L.; Yan, H.; Wang, X. J.; Zhao, Y. L., Light-Controllable Cucurbit[7]uril-based Molecular Shuttle. *J. Org. Chem.* **2012**, *77* (22), 10168-10175.
14. Buck, A. T.; Paletta, J. T.; Khindurangala, S. A.; Beck, C. L.; Winter, A. H., A Noncovalently Reversible Paramagnetic Switch in Water. *J. Am. Chem. Soc.* **2013**, *135* (29), 10594-10597.
15. Baroncini, M.; Gao, C.; Carboni, V.; Credi, A.; Previtera, E.; Semeraro, M.; Venturi, M.; Silvi, S., Light Control of Stoichiometry and Motion in Pseudorotaxanes Comprising a Cucurbit[7]uril Wheel and an Azobenzene-Bipyridinium Axle. *Chem.-Eur. J.* **2014**, *20* (34), 10737-10744.
16. Bergamini, G.; Fermi, A.; Marchini, M.; Locritani, M.; Credi, A.; Venturi, M.; Negri, F.; Ceroni, P.; Baroncini, M., A Highly Luminescent Tetramer from a Weakly Emitting Monomer: Acid- and Redox-Controlled Multiple Complexation by Cucurbit[7]uril. *Chem.-Eur. J.* **2014**, *20* (23), 7054-7060.
17. Fathalla, M.; Strutt, N. L.; Barnes, J. C.; Stern, C. L.; Ke, C. F.; Stoddart, J. F., Fluorescence Enhancement of a Porphyrin-Viologen Dyad by Pseudorotaxane Formation with Cucurbit uril. *Eur. J. Org. Chem.* **2014**, *2014* (14), 2873-2877.
18. Benyettou, F.; Zheng, X.; Elacqua, E.; Wang, Y.; Dalvand, P.; Asfari, Z.; Olsen, J. C.; Han, D. S.; Saleh, N.; Ehabiri, M.; Weck, M.; Trabolsi, A., Redox-Responsive Viologen-Mediated Self-Assembly of CB[7]-Modified Patchy Particles. *Langmuir* **2016**, *32* (28), 7144-7150.
19. Chen, Y. Y.; Huang, Z. H.; Xu, J. F.; Sun, Z. W.; Zhang, X., Cytotoxicity Regulated by Host Guest Interactions: A Supramolecular Strategy to Realize Controlled Disguise and Exposure. *ACS Appl. Mater. & Interfaces* **2016**, *8* (35), 22780-22784.
20. Du, J. W.; Zhang, P.; Zhao, X.; Wang, Y. X., An Easy Gene Assembling Strategy for Light-Promoted Transfection by Combining Host-guest Interaction of Cucurbit[7]uril and Gold Nanoparticles. *Sci. Rep.* **2017**, 7. DOI: 10.1038/s41598-017-06449-9
21. Samanta, S. K.; Brady, K. G.; Isaacs, L., Self-assembly of Cucurbit[7]uril Based Triangular Molecular Necklaces and Their Fluorescence Properties. *Chem. Commun.* **2017**, *53* (18), 2756-2759.
22. Cheng, Q.; Yin, H.; Rosas, R.; Gigmes, D.; Ouari, O.; Wang, R.; Kermagoret, A.; Bardelang, D., A pH-driven Ring Translocation Switch against Cancer Cells. *Chem. Commun.* **2018**, *54* (98), 13825-13828.
23. Shi, H.; Zhang, K.; Lin, R. L.; Sun, W. Q.; Chu, X. F.; Liu, X. H.; Liu, J. X., pH-Controlled Multiple Interconversion between Cucurbit[7]uril-based Molecular Shuttle, [3]Pseudorotaxane and [2]Pseudorotaxane. *Asian J. Org. Chem.* **2019**, *8* (3), 339-343.
24. Tcyrulnikov, N. A.; Varadharajan, R.; Tikhomirova, A. A.; Pattabiraman, M.; Ramamurthy, V.; Wilson, R. M., Modulation of Reduction Potentials of Bis(pyridinium)alkane Dications through Encapsulation within Cucurbit[7]uril. *J. Org. Chem.* **2019**, *84* (13), 8759-8765.
25. El-Barghouthi, M. I.; Assaf, K. I.; Rawashdeh, A. M. M., Molecular Dynamics of Methyl Viologen-Cucurbit[n]uril Complexes in Aqueous Solution. *J. Chem. Theory & Comp.* **2010**, *6* (4), 984-992.
26. Sindelar, V.; Silvi, S.; Kaifer, A. E., Switching a Molecular Shuttle On and Off: Simple, pH-controlled Pseudorotaxanes Based on Cucurbit[7]uril. *Chem. Commun.* **2006**, (20), 2185-7.
27. Kaifer, A. E.; Li, W.; Silvi, S.; Sindelar, V., Pronounced pH Effects on the Kinetics of Cucurbit[7]uril-based Pseudorotaxane Formation and Dissociation. *Chem. Commun.* **2012**, *48* (53), 6693-6695.
28. Kaifer, A. E., Portal Effects on the Stability of Cucurbituril Complexes. *Isr. J. Chem.* **2018**, *58* (3-4), 244-249.
29. Neira, I.; Garcia, M. D.; Peinador, C.; Kaifer, A. E., Terminal Carboxylate Effects on the Thermodynamics and Kinetics of Cucurbit[7]uril Binding to Guests Containing a Central Bis(Pyridinium)-Xylylene Site. *J. Org. Chem.* **2019**, *84* (4), 2325-2329.
30. Day, A.; Arnold, A. P.; Blanch, R. J.; Snushall, B., Controlling Factors in the Synthesis of Cucurbituril and its Homologues. *J. Org. Chem.* **2001**, *66* (24), 8094-8100.
31. Yi, S.; Kaifer, A. E., Determination of the Purity of Cucurbit[n]uril (n=7, 8) Host

Samples. *J. Org. Chem.* **2011**, *76* (24), 10275-10278.
32. Jeon, W. S.; Moon, K.; Park, S. H.; Chun, H.; Ko, Y. H.; Lee, J. Y.; Lee, E. S.; Samal, S.; Selvapalam, N.; Rekharsky, M. V.; Sindelar, V.; Sobransingh, D.; Inoue, Y.; Kaifer, A. E.; Kim, K., Complexation of Ferrocene Derivatives by the Cucurbit[7]uril Host: A Comparative Study of the Cucurbituril and Cyclodextrin Host Families. *J. Am. Chem. Soc.* **2005**, *127* (37), 12984-9.
33. Rekharsky, M. V.; Mori, T.; Yang, C.; Ko, Y. H.; Selvapalam, N.; Kim, H.; Sobransingh, D.; Kaifer, A. E.; Liu, S.; Isaacs, L.; Chen, W.; Moghaddam, S.; Gilson, M. K.; Kim, K.; Inoue, Y., A Synthetic Host-guest System Achieves Avidin-biotin Affinity by Overcoming Enthalpy-Entropy Compensation. *Proc. Nat. Acad. Sci. USA* **2007**, *104* (52), 20737-42.
34. Mock, W. L.; Shih, N. Y., Organic Ligand-Receptor Interactions between Cucurbituril and Alkylammonium Ions. *J. Am. Chem. Soc.* **1988**, *110*, 4706-4710.
35. Liu, S.; Ruspic, C.; Mukhopadhyay, P.; Chakrabarti, S.; Zavalij, P. Y.; Isaacs, L., The Cucurbit[n]uril Family: Prime Components for Self-Sorting Systems. *J. Am. Chem. Soc.* **2005**, *127* (45), 15959-15967.
36. Senler, S.; Cheng, B.; Kaifer, A. E., Rotaxane Formation by Cucurbit[7]uril in Water and DMSO Solutions. *Org. Lett.* **2014**, *16* (22), 5834-5837.
37. Appel, E. A.; Biedermann, F.; Hoogland, D.; del Barrio, J.; Driscoll, M. D.; Hay, S.; Wales, D. J.; Scherman, O. A., Decoupled Associative and Dissociative Processes in Strong yet Highly Dynamic Host-Guest Complexes. *J. Am. Chem. Soc.* **2017**, *139* (37), 12985-12993.
38. Hou, C. X.; Zeng, X. Z.; Gao, Y. Z.; Qiao, S. P.; Zhang, X.; Xu, J. Y.; Liu, J. Q., Cucurbituril As A Versatile Tool to Tune the Functions of Proteins. *Isr. J. Chem.* **2018**, *58* (3-4), 286-295.
39. Zhang, X. J.; Xu, X. Q.; Li, S. K.; Wang, L. H.; Zhang, J. X.; Wang, R. B., A Systematic Evaluation of the Biocompatibility of Cucurbit[7]uril in Mice. *Sci. Rep.* **2018**, *8*. DOI: 10.1038/s41598-018-27206-6
40. Zou, L.; Braegelman, A. S.; Webber, M. J., Spatially Defined Drug Targeting by in Situ Host-Guest Chemistry in a Living Animal. *ACS Central Science* **2019**, *5* (6), 1035-1043.
41. Chen, J. Z.; Zhao, G. Y.; Chen, L. M., Efficient Production of 5-Hydroxymethylfurfural and Alkyl Levulinate from Biomass Carbohydrate Using Ionic Liquid-based Polyoxometalate Salts. *Rsc Adv.* **2014**, *4* (8), 4194-4202.
42. Ahmed, R. M.; Hamdan, T. A.; Numan, A. T.; Al-Jeboori, M. J.; Potgieter, H., Formation of Polymeric Assemblies of Six-coordinate Metal Complexes with MixedBbridges of Dicarboxylato-azido Moieties. *Complex Metals* **2014**, *1* (1), 38-45.
43. Wang, P. P.; Wu, Y. L.; Zhao, Y. X.; Yu, Y.; Zhang, M. M.; Cao, L. P., Crystalline Nanotubular Framework Constructed by Cucurbit[8]uril for Selective CO_2 Adsorption. *Chem. Commun.* **2017**, *53* (40), 5503-5506.
44. Sun, Y. Q.; Zhang, J.; Ju, Z. F.; Yang, G. Y., Two-dimensional Noninterpenetrating Transition Metal Coordination Polymers with Large Honeycomb-like Hexagonal Cavities Constructed from a Carboxybenzyl Viologen Ligand. *Cryst. Growth Des.* **2005**, *5* (5), 1939-1943.
45. Wang, H. Y.; Zhang, H., A Novel Photochromic Cadmium Coordination Polymer Based on a New Viologen Ligand Accompanying Photoswitchable Luminescence Properties. *Inorg. Chem. Commun.* **2019**, *102*, 240-244.
46. Wang, S. X.; He, W. J.; Xiao, C. S.; Tao, Y. H.; Wang, X. H., Synthesis of Y-Shaped OEGylated Poly(amino acid)s: The Impact of OEG Architecture. *Biomacromolecules* **2019**, *20* (4), 1655-1666.
47. Gong, T.; Yang, X.; Fang, J. J.; Sui, Q.; Xi, F. G.; Gao, E. Q., Distinct Chromic and Magnetic Properties of Metal Organic Frameworks with a Redox Ligand. *ACS Appl. Mater. & Interfaces* **2017**, *9* (6), 5503-5512.